Eur. Phys. J. D **11**, 295–300 (2000)

THE EUROPEAN PHYSICAL JOURNAL D

EDP Sciences
© Società Italiana di Fisica
Springer-Verlag 2000

X-ray emission from aluminium under intense, ultrashort irradiation

S. Banerjee, G. Ravindra Kumar[a], and L.C. Tribedi

Tata Institute of Fundamental Research, Homi Bhabha Road, Bombay 400 005, India

Received 12 August 1999 and Received in final form 29 November 1999

Abstract. We present studies of X-ray emission from aluminium under picosecond and femtosecond irradiation in the intensity range $\sim 10^{12}$–10^{15} W cm^{-2}. We use a new and simple method to measure *spectrally* resolved absolute X-ray yields. It is shown that the X-ray yields can be obtained for arbitrary levels of X-ray flux. We present details of the variation of the absolute yields as a function of wavelength, intensity, polarization and pulse duration of the incident laser radiation. Electron temperatures in the keV range are observed at 10^{15} W cm^{-2} with femtosecond laser pulses.

PACS. 52.25.Nr Emission, absorption, and scattering of X and γ-radiation – 52.40.Nk Laser-plasma interactions (e.g., anomalous absorption, backscattering, magnetic field generation, fast particle generation) – 52.50.Jm Plasma production and heating by laser beams

1 Introduction

There is currently tremendous interest in the study of coherent and incoherent emission in the vacuum ultraviolet (VUV) and X-ray regions induced by intense, ultrashort laser pulses [1–3]. Some of the exciting aspects that have so far been studied in ultrashort laser produced plasmas include the high charge densities, keV–MeV electron temperatures, possibility of producing giga-gauss magnetic fields and non-Maxwellian particle distributions, characteristic of matter subjected to extreme levels of excitation. X-ray emission has been a crucial experimental probe in the study of such plasmas.

Apart from the interest in the fundamental aspects of laser-matter interaction relevant to such intense excitation, the potential for making practical ultrashort pulsed light sources in these spectral regions [4] makes such studies attractive from the point of view of applications in chemical and biological dynamics [5,6], X-ray lasers [7] and so on. X-ray emission is a very useful diagnostic of the plasma properties that complements other methods which measure the characteristics of charged particle or optical emission from such plasmas. The dependence of the X-ray emission on the characteristics of the exciting laser can be used to understand the coupling of the input laser light to the plasma as well as its relaxation dynamics [1,5,8–10]. Since there are many channels available both in the excitation and relaxation processes, it is essential to determine the contribution of each channel and understand the competition among them [11]. It is thus very important to get a reliable measure of the absolute yields of the emitted X-rays. The standard methods of measuring X-ray yields [12–18] however, involve a number of steps each of which can contribute its own errors to the final estimates. We use a recently proposed technique [19] to measure the absolute X-ray yields and use them to understand the behaviour of aluminium plasma produced with intense picosecond and femtosecond radiation. Our experimental method enables us to obtain spectrally resolved X-ray yields as a function of the incident wavelength, intensity, pulse duration and light polarization. Considerable efficiency for X-ray emission at intensities as low as 10^{13} W cm^{-2} is observed in our studies. The physics governing the X-ray emission process is examined.

2 Experimental details

2.1 Laser systems

The experimental set up used is shown in Figure 1. Radiation from a picosecond Nd-YAG and a femtosecond Ti-sapphire lasers incident on high purity metal targets have been used to produce high density plasmas in our experiments. The picosecond pulses were provided by a hybrid mode locked Nd-YAG laser that emits 35 ps pulses at 1064 nm, 532 nm and 355 nm at a repetition rate of 10 Hz. The maximum pulse energy at 1064 nm is 70 mJ. The femtosecond light pulses were obtained from a custom built chirped pulse amplification (CPA) Ti-sapphire laser system, consisting of two amplification stages. It produces a maximum of 50 mJ/pulse at 806 nm with a pulse duration of 100 fs and repetition rate of 10 Hz. For the present experiments, the maximum was pegged at 20 mJ.

[a] e-mail: grk@tifr.res.in

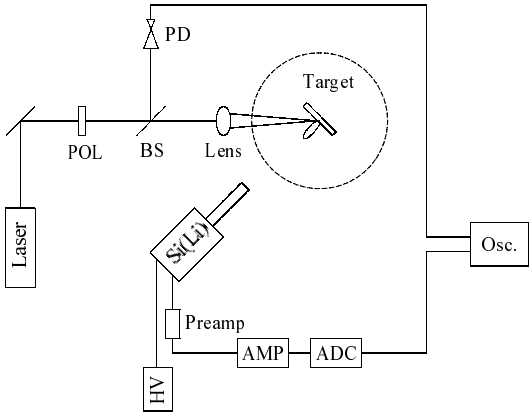

Fig. 1. Experimental setup used. POL: polarizer, QWP: quarter waveplate (optional), BS: beam splitter, PD: photodiode and MCA: multichannel analyser.

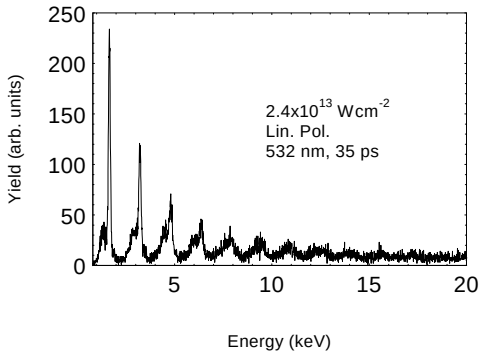

Fig. 2. X-ray spectra from Aluminium with 532 nm, 35 ps pulses at 2.4×10^{13} W cm^{-2}. The laser light is linearly polarized (s-polarization).

Two kinds of polarization were used in the experiment – linear (S) polarization and circular polarization. A high quality polarizer was inserted in the beam before focusing to ensure s-polarization. For experiments which needed circular polarization, a thin quarter wave plate was introduced after the polarizer. The laser pulses were focussed onto a metal target using biconvex lenses of different focal lengths $f = 10$, 15 and 20 cm. The focussed spot diameter was measured by the scanning knife edge method. Typically the value of the spot size at the focus is 20 μm for $f = 10$ cm and 25 μm for $f = 20$ cm at 1064 nm. The target was mounted in a chamber evacuated to 10^{-3} torr. The solid target, in the form of a disc was continuously rotated and translated using a stepper motor drive to ensure the exposure of fresh target regions to laser light.

2.2 X-ray detection

Our method uses a simple solid state detector, well-known for its reasonably good resolution and high efficiency, and extensively used in experimental nuclear and atomic physics. In the latter experiments, the flux of emitted X-rays is small and the detection process is relatively uncomplicated since in each event at most one X-ray photon is detected. Ultrashort laser produced plasmas, however, emit large fluxes of radiation which are temporally short. As such the detector would see very short "bursts" of X-ray photons. Since the detector is energy sensitive, the output pulse height would be proportional to the total energy deposited. Special care therefore needs to be taken to correctly estimate the yield when such detectors are used. We will show that this is relatively easy and one obtains reliable measures of the absolute X-ray yield in a simple fashion.

The X-ray emission from the plasma was measured by a liquid nitrogen cooled (77 K) Si(Li) detector (Canberra) having a $\sim$ 25 μm beryllium window. The output was amplified and recorded on a multichannel analyser using an ADC unit. The pulse height was calibrated using standard radioactive sources. The detector has a range of 1–20 keV [20] and a resolution of 160 eV at 1.6 keV. The X-ray emission was detected through an equally thick mylar window on the vacuum chamber. Spectra were collected typically over 20 000–30 000 laser shots. The shortest target-detector distance was 4 cm and the detector surface area was 0.3 cm^{-2} giving a maximum solid angle of 0.02 sr for the collection. The detector was placed along the plasma plume direction (normal to the target surface). The target was mounted at an angle of 45° with respect to the input laser beam. The X-ray yield was corrected for the efficiency of the detector, absorption in the beryllium and mylar windows and the size of the solid angle sampled in the experiment. The last was done assuming an isotropic distribution and thus the measured yields were multiplied by 2π. Unlike in other measurements where the X-ray flux arriving at the detector must be below some limit so as to ensure correct measurement of the incident flux, our scheme suffers from no such restrictions and can handle arbitrarily large X-ray fluxes.

3 Results and discussion

3.1 Picosecond laser excitation

Figure 2 shows a typical spectrum obtained from aluminium under irradiation by a 532 nm, 2.4×10^{13} W cm^{-2}, s-polarized laser field. The spectrum consists of a series of peaks, with the first peak occurring at $\sim$ 1.6 keV, a value which can be understood as the characteristic K-X-ray from highly charged Al ions (the normal K-X-ray, which is due to a single vacancy, is at 1.5 keV). The other peaks occur at energies which are integral multiples of the energy of the first peak. The highest peak which could be clearly resolved occurs at 14.4 keV, corresponding to 9 times the energy of the first peak.

Examination of such spectra taken over many runs and under different incident light field parameters revealed that the multiple peak structure was a consequence of the simultaneous arrival of more than one photon at the detector in a time short compared to the temporal resolution

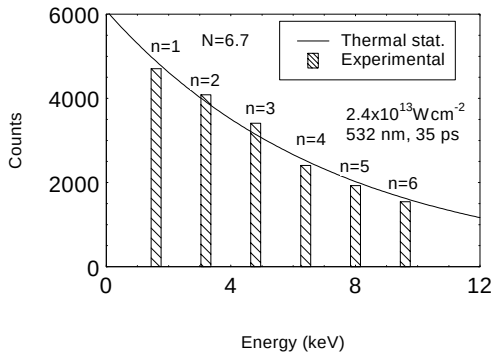

Fig. 3. Fits to the data in Figure 2 assuming the plasma to be a thermal source. The histograms represent areas under the curve after appropriate corrections as mentioned in the text. The solid curve is based on thermal statistics with $N = 6.7$.

of the detector. This is a peculiar aspect of such energy sensitive detectors for experiments where many photons, each possessing the same energy, can arrive simultaneously at the detector. Care must, therefore, be exercised in estimating the total yields of X-rays measured using such a detection system. To explain further, after excitation of the solid target by a particular laser shot, two or more X-ray photons may simultaneously arrive at the detector [19,21]. Such bursts are common from high luminosity sources like laser produced plasmas, but unlikely to be encountered in a typical ion-atom or electron-atom collision experiment where the X-ray production is not so copious. The duration of the emitted X-ray pulse in our case is expected to be of the order of the input pulse duration (1–10^2 ps) [1,22], which is a small fraction of the detector response time (typically ns-μs, see [23]). The detector perceives "p" such closely timed photons as if they were one photon of "p" times the energy, resulting in a peak at "p" times the basic X-ray photon energy [19,21]. The total X-ray yield is obtained by integrating the area under each peak and adding up these areas after multiplying by the appropriate number (2 for the second peak, 3 for the third peak and so on).

Since the characteristic X-rays produced from a laser produced plasma are expected to be incoherent we have fitted the experimentally obtained spectra to the Bose-Einstein distribution [24]

$$P(n) = \frac{1}{(1+N)}\left[\frac{N}{(N+1)}\right]^n. \qquad (1)$$

The parameter N is the average photon number given by $(1/\mathrm{e}^{-h\nu/kT} - 1)$. Experimentally this quantity depends on the source strength.

Using the above equation, we analyse the data shown in Figure 2. The figure shows that the data are well fitted by Bose-Einstein statistics. It turns out that the best fit is obtained for $N = 6.7$ (see Fig. 3). We have obtained consistent fits to different sets of data using the above distribution. Once the fits are obtained, we can calculate the total X-ray yield. We have obtained fits to data for different laser parameters which corresponds to different X-ray luminosity and find that good fits are obtained for almost all sets of data. We have also noticed that under low luminosity the higher peaks vanish, as expected. It is to be noted that this procedure is very simple for the case of a single emission line. In the case of a continuous distribution like Bremsstrahlung, the treatment becomes more complicated.

The above fitting procedure also helps in identifying the proper spectral features. For example, if a "true" peak is present at a higher energy, where there is a higher order contribution from a lower energy peak, the correct strength of the "true" peak can be ascertained by subtracting the contribution of the lower energy peak from the total. It is in the estimate of the higher order contribution that the statistics assume significance. It is to be noted that, the distribution allows us to estimate the higher order contributions that are buried in noise. We can even get an idea of the number of peaks that we really need to consider in order to get a good signal to noise ratio and estimate the errors associated with the contributions we ignore.

As an example, let us consider Figure 3 again and estimate the error associated with a measurement when neglecting different higher energy peaks. These values turn out to be 10% for neglecting $n = 6$ and above, 20% for neglecting $n = 5$ and above, 30% for neglecting $n = 4$ and above and so on. We thus get a reliable estimate of the errors involved in measuring the absolute yields, particularly when the higher energy peaks are barely above the noise/background level in the detector.

We wish to emphasize the simplicity and versatility of our detection scheme in contrast to the usual methods of measuring X-ray yields [12–18]. The usual methods involve a dispersive element (grating or crystal) followed by a detector (X-ray film/electronic); the latter either works in particle counting mode or in current integration mode. The losses in the dispersive elements have to be carefully estimated before the yields can be estimated; besides these losses (grating reflectivites, input/output slit transmission) are themselves a function of time and could change for different experimental runs. The energy range of dispersive elements is usually small (to ensure high spectral resolution) and different gratings/crystals are needed for different spectral regions. Moreover, detectors working in the particle counting mode can, at the most, sense one X-ray photon per detection event. The fluxes thus have to be kept at a low level by attenuating filters before the detector – these filters again have to be calibrated properly. In the case of photographic film its calibration has to be done carefully to obtain the absolute yield. There are conventional methods which eliminate the dispersive element (like p-i-n diodes, dosimeters) but they give only *spectrally integrated* yields. In contrast, our detection scheme gives (a) spectral information, (b) does not restrict the X-ray flux entering the detector (c) has only a single stage and most importantly (d) measures the absolute yield with near unit efficiency.

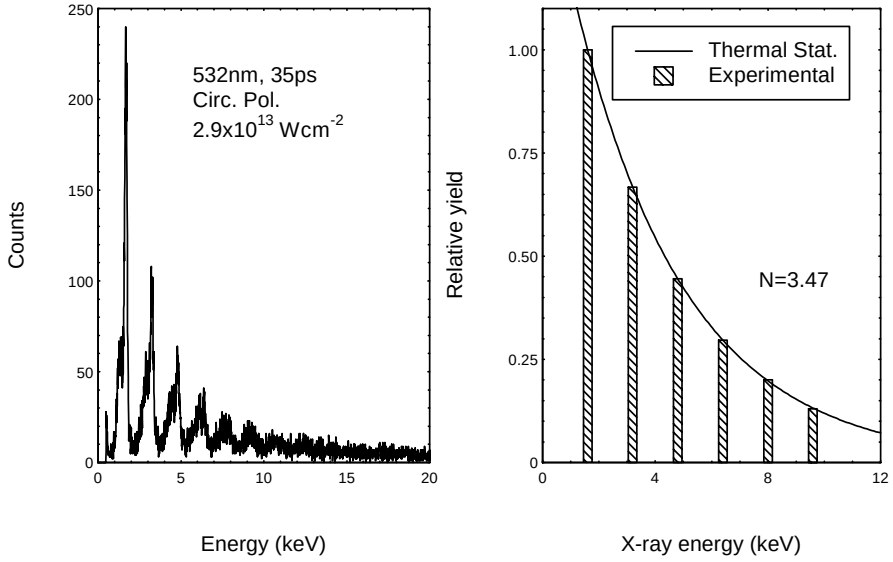

Fig. 4. Left: X-ray spectra from Aluminium with 532 nm, 35 ps pulses at 2.9×10^{13} W cm^{-2}. The laser light is circularly polarized. Right: yields with a fit based on Bose-Einstein statistics with $N = 3.5$.

Let us now move on to discuss the observations of X-ray yield as a function of different laser parameters. Figure 4 presents data on the X-ray yield for a circularly polarised laser light at 532 nm at an intensity of 2.9×10^{13} W cm^{-2}. The raw spectrum shows seven discernible peaks, in contrast to nine that appear in the case of *s*-polarised laser light (Fig. 2). The smaller number of peaks in itself indicates less X-ray flux, as per the discussion above. The fit based on Bose-Einstein statistics clearly establishes that it is so, with a value of $N = 3.5$ (compare Fig. 4, for which $N = 6.7$). The yield thus decreases when the polarization is circular. The total K-X-ray yield for the linearly polarized case is 1.3×10^5 over $\sim 65\,000$ laser shots, giving a yield of ~ 2.0 K-X-ray photons per shot. The corresponding figure for the circularly polarized case is 1.6. Note that since the counts have been obtained over a very large number of shots, the statistical error is negligible in the X-ray yield per laser shot. It is clear that even though the circularly polarized light intensity is marginally stronger than the corresponding value for linearly polarized light, the X-ray yields are considerably lower. This observation is in contrast to other recent reports (although those experiments used a gas target) that circular (elliptical) polarization enhanced the X-ray yield at intensities of 10^{15} W cm^{-2}[25]. These observations were explained on the basis of a higher plasma density caused by higher kinetic energies of the ionized electrons in the tunneling regime. We can offer a tentative conjecture to explain our observations of decreased yield. It is known that circular polarization is less effective in causing multiphoton ionization at moderately intense fields like those used in our experiment at 532 nm [26]. We can thus assume that the plasma that is formed in the circularly polarized field is less dense than that in the linearly polarised field. The lower densities give rise to decreased X-ray emission. It is also possible that the reflectivity of the plasma in the two cases may have a role to play in the coupling of the light into the plasma. The reabsorption of the emitted X-rays could also be different in the two cases. These need to be investigated further.

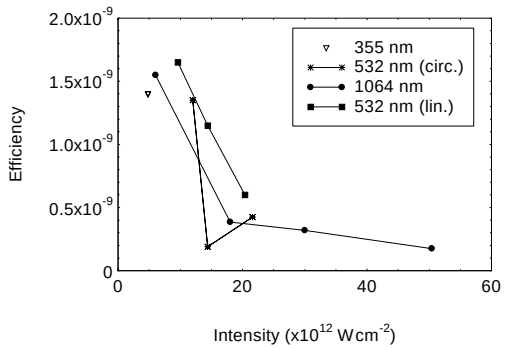

Fig. 5. Variation of absolute X-ray yields with laser intensity for different wavelengths and polarizations. The laser light is *s*-polarized

It is also interesting to note that the X-ray spectra, even under the present resolution (which is of the order of 10^2 eV at best) can still give information about the charge states present. In the linear polarization case at 532 nm (Fig. 2), the K-X-ray peak occurs at 1.68 keV. The X-ray peak for an ion with a single vacancy in the K-shell is expected at 1.50 keV. The "blue" shift of 0.18 keV is due to the high ionization state of aluminium ions emitting the X-ray. This corresponds to a most probable charge states of $Al^{11+,12+}$ [27]. Similar charge states are also created by circularly polarized case at 532 nm. The dependence of charge states on a wavelength, intensity and pulse duration will be discussed a little later.

Figure 5 presents the K-X-ray yield from aluminium as a function of intensity for different laser wavelengths. The laser radiation in all the cases is *s*-polarized. We notice that except at 355 nm where detailed data were not obtained, the efficiency for conversion into the K-X-ray decreases as a function of the input energy. The conversion efficiency is defined as the ratio of the total X-ray energy yield to the input laser pulse energy per laser shot. The maximum efficiency for conversion into the K-X-ray

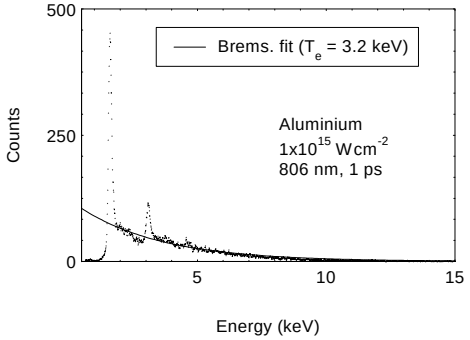

Fig. 6. X-ray spectrum from aluminium with 806 nm, 1 ps, *s*-polarized pulses. $I = 1.0 \times 10^{15}$ W cm^{-2}. The solid line is a fit to the Bremsstrahlung component with a temperature of 3.2 keV.

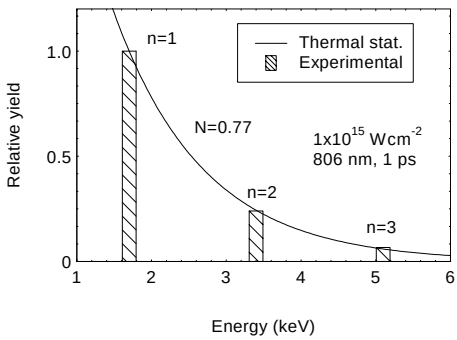

Fig. 7. Photon statistics analysis of the K-X-ray yield of aluminium for the data in the previous figure.

of aluminium was found at 532 nm for linearly polarised light and it turned out to be 3.4×10^{-9}. Note that this is just the conversion into the K-X-ray channel. The decrease in the efficiency can be attributed to increased reflection and inefficient coupling of the laser energy into the plasma at high intensities.

3.2 Femtosecond laser excitation

Figure 6 shows the data obtained with 1 ps *s*-polarized laser pulse excitation at 806 nm (the femtosecond laser was operated at 1 ps for this part of the experiments). The excitation intensity here is one to two orders of magnitude larger than those derived from the Nd-YAG laser. An obvious difference between the spectrum in this figure and those obtained with picosecond excitation (Figs. 2 and 4) is the appearance of a background that peaks at zero and decays at higher X-ray energies. The characteristic K-X-ray emission peaks are superposed on this background. The background is due to Bremsstrahlung radiation emitted by the plasma. An exponential fit (solid curve in Fig. 6) to the data gives an electron temperature of 3.2 keV. The Bremsstrahlung yield integrated over the entire spectral range corresponds to a value of 0.3 counts per laser shot, indicating that pile-up effects in the Bremsstrahlung component of the spectrum are insignificant and hence a reliable estimate of the electron temperature can be made.

We can subtract the Bremsstrahlung contribution from the overall signal and obtain the signal due to the characteristic K-X-ray. We have fitted the Bose-Einstein statistics with $N = 0.8$ to the characteristic K-X-ray part of the spectrum (Fig. 7). The fit obtained is quite satisfactory and demonstrates that it is possible to estimate absolute characteristic X-ray yields even in the presence of other overlapping emission signals. From the spectra at different intensities, we also know that Bremsstrahlung contribution increases and the characteristic X-ray emission decreases as the laser intensity goes up. Figure 8 shows the emission at the marginally higher intensity for a 100 fs pulse at the same wavelength. This figure clearly indicates

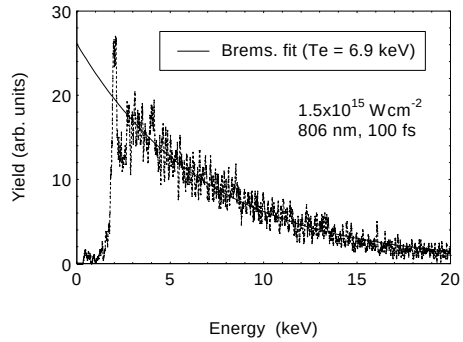

Fig. 8. X-ray emission spectrum from aluminium with 806 nm, 100 fs, *s*-polarized pulses at an intensity of 1.5×10^{15} W cm^{-2}. The solid curve is a Bremsstrahlung fit with an electron temperature of 6.9 keV.

the dominant role of Bremsstrahlung at the higher intensity; the characteristic K-X-ray emission is almost masked by Bremsstrahlung. The higher electron temperature here can be understood to be due to more efficient excitation by the shorter pulse [15].

An aspect that needs to be investigated further is the estimation of absolute Bremsstrahlung spectrum using the Si(Li) detector for the purpose of measuring the electron temperature. The complication here is that there is no characteristic line energy whose multiples can be taken to indicate the arrival of multiple photons at the detector. We are working on a method to apply the statistics to such a continuous spectrum.

The X-ray spectra also contain information on the charge state distribution of the aluminium ions in the plasma as has been discussed previously. As we discussed above, the energy of the emitted X-ray is blue shifted – the magnitude of the shift depends on the most probable charge state, higher charge states producing larger shifts. Figure 9 shows the peak position of the K-X-ray as function of various laser parameters. For lower intensities and longer pulses the blue shift is about 160 eV which is consistent with the most probable charge state being Al^{11+}. At higher intensities and with shorter pulses the shift increases to 200 eV. For the shortest pulses (100 fs) and highest intensities accessed in our experiment the shift

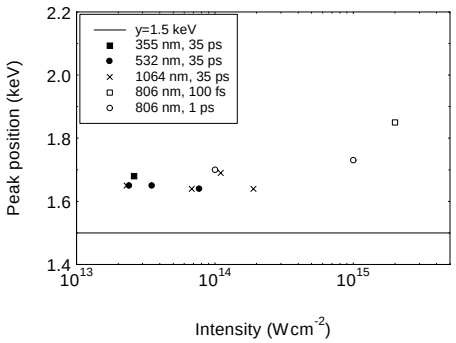

Fig. 9. Peak position of the characteristic K-X-ray emission as a function of various laser parameters with *s*-polarized excitation. Note the larger blue shift for higher intensities and shorter pulses.

is greater than 300 eV corresponding to a most probable charge state of Al^{12+}. It is of interest to note that for similar intensities the shift is larger for temporally shorter pulses. A larger blue shift is accompanied by a corresponding increase in the electron temperature form 3.2 to 6.9 keV when the pulse duration decreases from 1 ps to 100 fs. These observations are consistent with the fact that ionization is more efficient with shorter pulses.

In conclusion, we have measured absolute X-ray yields from aluminium irradiated by picosecond and femtosecond laser pulses with peak intensities in the range $10^{14}-10^{16}$ W cm^{-2}. We have pointed out the role of photon statistics in the interpretation of the data and demonstrated a simple and easy method that enables a quick measurement of yields. We have discussed the dependence of the absolute X-ray yield on the laser polarization, wavelength, intensity and pulse duration. We observe suppression of characteristic X-ray emission with circular polarization of the laser input. We have observed keV electron temperatures with 100 fs pulses at 10^{15} W cm^{-2} and charge states as large as Al^{12+}. The relative ease with which absolute yields can be measured by our method should help in attaining a better understanding the excitation and relaxation mechanisms in laser produced plasmas.

The TIFR high energy, femtosecond laser facility has been set up with substantial funding from the Department of Science and Technology, Government of India. We thank Amal K. Saha for his participation in some of the experiments and Riju C. Issac for constructive suggestions.

References

1. M. Murnane, H. Kapteyn, M.D. Rosen, R. Falcone, Science **251**, 531 (1991).
2. R.M. More, *Laser Interactions with Atoms, solids and Plasmas* (NATO ASI Series B Plenum Press, New York, 1994), Vol. 327.
3. S.J. Rose, *Laser Interaction with Matter* (Institute of Physics Conference Series, No. 140, IOP Publishing, Bristol, 1997).
4. A. Rousse, P. Audebert, J.P. Geindre, F. Fallis, J.C. Gauthier, A. Mysyrowicz, G. Grillon, A. Antonetti, Phys. Rev. E **50**, 2200 (1994).
5. *High Fields and Short Wavelength Generation*, Spl. issues, J. Opt. Soc. Am. B **13**, Nos. 1 and 2 (1996).
6. C. Rischel, A. Rousse, I. Uschmann, P.A. Albuoy, J.-P. Geindre, P. Audebert, J.-C. Gauthier, E. Forster, J.-L. Martin, A. Antonetti, Nature **390**, 490 (1997) and references therein.
7. C. Yamanaka, *Short Wavelength Lasers and their Applications* (Springer Proceedings in Physics, Springer-Verlag, 1988), Vol. 30.
8. E.M. Campbell, Phys. Fluids B **4**, 3781 (1992).
9. P. Gibbon, E. Forster, Plasma Phys. Control. Fusion **38**, 769 (1996).
10. D. Riley, O. Willi, S.J. Rose, T. Afshar-Rad, Europhys. Lett. **10**, 135 (1989).
11. U. Teubner, T. Missalla, I. Uschmann, E. Forster, W. Theobald, C. Ulker, Appl. Phys. B **62**, 213 (1996); D. Altenbernd, U. Tuebner, P. Gibbon, E. Forster, P. Audebert, J.-P. Giendre, J.C. Gauthier, G. Grillon, A. Antonetti, J. Phys. B **30**, 3969 (1997).
12. D.G. Stearns, O.L. Landen, E.M. Campbell, J.H. Scofield, Phys. Rev. A **37**, 1684 (1988).
13. J.A. Cobble, G.A. Kyrala, A.A. Hauer, A.J. Taylor, C.C. Gomez, N.D. Delamater, G.T. Schappert, Phys. Rev. A **39**, 454 (1989).
14. M. Chaker, J.C. Kieffer, J.P. Matte, H. Pepin, P. Audebert, P. Maine, D. Strickland, P. Bado, G. Mourou, Phys. Fluids. B **3**, 167 (1991).
15. P. Audebert, J.P. Geindre, J.C. Gauthier, A. Mysyrowicz, J.P. Chambaret, A. Antonetti, Europhys. Lett. **19**, 189 (1992).
16. H. Chen, B. Soom, B. Yakobi, S. Uchida, D.D. Meyerhofer, Phys. Rev. Lett. **70**, 3431 (1993).
17. D.D. Meyerhofer, H. Chen, J.A. Delettrez, B. Soom, S. Uchida, B. Yakobi, Phys. Fluids. B **5**, 2584 (1993).
18. B.N. Chichkov, C. Momma, A. Tunermann, S. Meyer, T. Menzel, B. Wellegehausen, Appl. Phys. Lett. **68**, 2804, 1996.
19. S. Banerjee, G. Ravindra Kumar, A.K. Saha, L.C. Tribedi, Opt. Commun. **158**, 72 (1998).
20. L.C. Tribedi, P.N. Tandon, Nucl. Instrum. Meth. B **69**, 178 (1992).
21. S. Dobosz, M. Lezius, M.Schmidt, P. Meynadier, M. Perdrix, D. Normand, J.-P. Rozet, D. Vernhet, Phys. Rev. A **56**, R2526 (1997).
22. D.W. Phillion, C.J. Hailey, Phys. Rev. A **34**, 4886 (1986).
23. G.F. Knoll, *Radiation Detection and Measurement*, 2nd edn. (John Wiley & Sons, NY, 1989).
24. B.E.A. Saleh, M.C. Teich, *Fundamentals of photonics* (John-Wiley & Sons,Inc. New York, 1991), p 406; D. Marcuse, *Principles of Quantum Electronics* (Academic Press, NY, 1980).
25. G. Pretzler, E.E. Fill, Phys. Rev. E **56**, 2112 (1997).
26. P.H. Bucksbaum, M. Bashkansky, R.R. Freeman, T.J. McIlrath, L.F. Di Mauro, Phys. Rev. Lett. **56**, 2590 (1986); N.J. van Druten, R. Trainham, H.G. Muller, Phys. Rev. A **51**, R898 (1995).
27. B.K. Godwal, A. Ng, L. DaSilva, Y.T. Lee, D.A. Liberman, Phys. Rev. E **40**, 4521 (1989).